Chirality Information Transfer in Polylactides: From Main-Chain Chirality to Lamella Curvature

Damien Maillard and Robert E. Prud'homme*

Department of Chemistry, Université de Montréal, Pavillon J. A. Bombardier, 2900 Edouard Montpetit, H3T 1J4 Montreal, Quebec, Canada

Received February 10, 2006
Revised Manuscript Received March 17, 2006

Introduction. Poly(lactide)s are biodegradable and biocompatible polyesters produced from renewable carbon sources via cationic ring-opening polymerization.[1] They are found in three different enantiomeric forms: the D, the L, and the meso. D- and L-poly(lactide)s, PDLA and PLLA, respectively, are semicrystalline polymers, whereas the meso is amorphous.[2] Three crystalline states have been observed for PDLA and PLLA,[3] depending on the crystallization conditions: the α phase has been observed from solution or melt crystallization, whereas β and γ phases have been found in melt-extruded fibers or upon stretching.[4]

The α form has been found by X-ray diffraction to have a pseudo-orthorhombic $2_1 2_1 2_1$ unit cell with parameters $a = 1.07$, $b = 0.645$, and $c = 2.78$ nm,[5−7] its chains being arranged in a 10_3 helical conformation.[8−10] Solution-grown crystals of that state are lozenge-shaped, whereas crystals grown from the melt are hexagonal. Two different kinds of sectors have been identified in hexagonal crystals: four (110) sectors, equivalent to the four sectors of the lozenge-shaped crystals, and two (200) sectors.[11−14]

The influence of chirality, which is a molecular scale feature, on the macroscopic properties has been the subject of several studies. Nandi and Vollhardt[15] have reviewed the case of low molecular weight enantiomers and shown the chiral discrimination occurring in, for example, amino acid amphiphiles prepared in monolayers and visualized by Brewster angle microscopy; the direction of the main growth axes bears a mirror-image relationship for the enantiomers. Actually, this case is not very different from the initial observation of Pasteur, concerning tartaric acid crystals.[16] Similar examples of chiral discrimination have been found with phospholipids which exhibit condensed phase domains curving in opposite directions (clockwise and anticlockwise) for the two enantiomers, while the racemic mixture shows no curvature.[15] In the case of macromolecular crystals, lamellar twisting has been correlated with the chain chirality; in silk fibroin, for example, the crystal twist can be linked to the chirality of the peptide residue of the chain.[17] In synthetic polymers, Brown et al. have observed, in the case of a chiral polymer (polyepichlorohydrin), a link between the lamellar twist, which conducts to the banding of the spherulites, and the polymer chirality.[18] As a second example with synthetic polymers, Li et al. have shown, for a series of chiral polyesters, that all crystals have the same twist, and changing the handedness of the chiral center reverses the lamellar twist.[19−21] In that context, Lotz and Cheng[22] have proposed, following Keith and Padden,[23,24] that the curvature of polymer crystals is a consequence of chain folding, steric hindrance or chain tilt,[25] these parameters being influenced by the helical arrangement of the polymer (which is, in turn, controlled by the polymer chirality).

* Corresponding author. E-mail: re.prudhomme@umontreal.ca.

In this Communication, crystalline lamellae grown from ultrathin films of polylactide are observed by in situ AFM. It will be shown that PLLA and PDLA give rise to different curvatures depending on their molecular chirality.

Experimental Section. Poly(L-lactide) was provided from Polysciences Inc. and poly(D-lactide) from Purac Inc.; both were used without further purification. Their molecular weights were determined by gel permeation chromatography using a Wyatt light scattering detector: $M_n = 120\,000$ g mol^{-1} and polydispersity (PD) = 1.30 for the poly(D-lactide); $M_n = 110\,000$ g mol^{-1} and PD = 1.26 for the poly(L-lactide). The glass transition temperatures and melting points were determined using a Perkin-Elmer DSC-7 apparatus. For PLLA, $T_g = 57$ °C and T_f (maximum of the peak) = 176 °C; for PDLA, $T_g = 56$ °C and T_f (maximum of the peak) = 180 °C.

Ultrathin films were prepared by spin-coating at a rotation speed of 3000 rpm for 20 s, following an acceleration of 4000 rpm/s, using a Headway Research Inc. EC-101 apparatus. Dichloromethane was used as solvent. The film thickness was controlled by the solution concentration; concentrations from 2 up to 20 mg/mL were used to obtain thicknesses ranging between 5 and 100 nm. The films were cast onto cleaned Si substrates (p-type single side polished (100) silicon wafers). The wafers were cleaned by immersion in nitrohydrochloric acid for 1 h in an ultrasonic bath to remove any organic contamination and to hydroxylate the native oxide layer, thus making the surface hydrophilic. The substrates were then rinsed with distilled water and dried by spin-coating for 40 s at 3000 rpm, before treatment in a plasma cleaner (Harrick PDC-32G) at 18 W for 20 s. To keep a solvent-saturated atmosphere around the sample and to allow uniform evaporation, a glass dome was placed on top of the sample area during spin-coating. Film thicknesses were measured by atomic force microscopy.

A Nanoscope III multimode AFM apparatus (Digital Instruments (DI)), operated in tapping mode and equipped with a high-temperature heating accessory (DI), was used to capture images during isothermal crystallization at various temperatures. A JVH scanner was used (maximal scan size 130 × 130 μm) with silicon nitride probes (Nanosensor).

Spin-coated samples were melted in the AFM stage at 185 °C for 2 min. Then, the stage temperature was decreased to the chosen crystallization temperature. The surface was observed with a scan size of 50 × 50 μm and zoomed to observe more accurately some details. The scan rate was 1 Hz. Nucleation was induced by decreasing suddenly the AFM probe amplitude set point along one line to initiate a contact.

In the crystallization experiments, two parameters were varied: the film thickness (between 5 and 100 nm) and the crystallization temperature (between 125 and 165 °C). The latter was chosen to cover an interval containing the fastest crystallization rate, which was determined, from optical microscopy, to be at 135 °C.

Results. Figure 1 shows a series of AFM height pictures obtained with a PLLA film of 15 nm in thickness, kept at 145 °C.

Figure 1a shows the polymer surface shortly after the nucleation, initiated in the middle of the picture; the nucleation horizontal line is surrounded by flat-on and edge-on lamellae perpendicular to the line. In Figure 1b−d, we see more clearly the intertwining of flat-on and edge-on lamellae, growing with time (from Figure 1b to Figure 1d). In some instances, flat-on

10.1021/ma060316c CCC: $33.50
Published on Web 05/24/2006

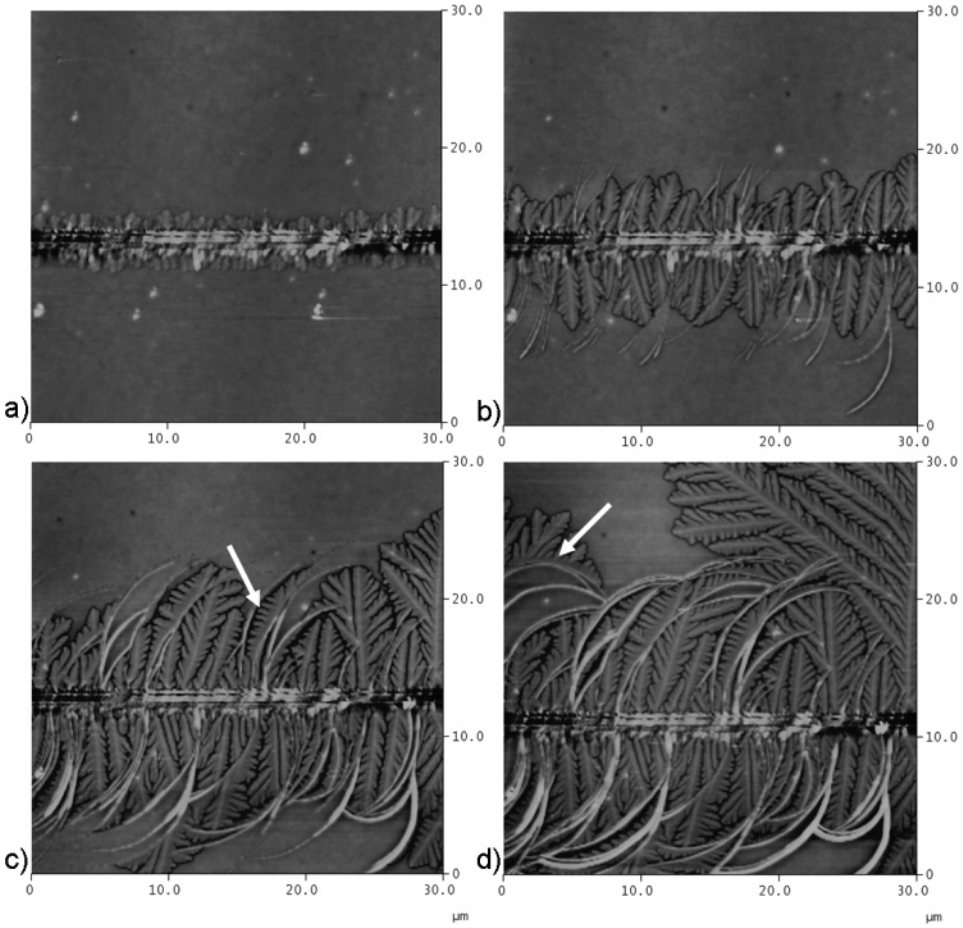

Figure 1. PLLA film with a thickness of 15 nm crystallized at 145 °C. The capture window has a 50 × 50 μm dimension: (a) has been taken 4 min 16 s, (b) 8 min 32 s, (c) 17 min 4 s, and (d) 42 min 40 s after nucleation. Edge-on crystals appear as curved S-shaped white threads.

lamellae are initiated by the middle line and grow parallel to the edge-on lamellae; in other instances, the flat-on lamellae are initiated by the edge-on lamellae, as indicated in Figure 1c,d by the arrows. The edge-on lamellae are growing in both directions, above and below the nucleation horizontal line, and quickly exhibit a S-shaped curvature.

Figure 1 is representative of the morphology observed for all the films investigated and for all crystallization temperatures (but the kinetics varies greatly with the temperature). The only variation between the different thicknesses and crystallization temperatures is the density of edge-on lamellae. In all cases, the growth of edge-on lamellae stops at 10−20 μm from the nucleation point. In the case of low lamella density, the edge-on crystal growth is stopped by the flat-on crystal expansion which "strangles" them; in the case of high lamella density, the edge-on crystal growth stops because of the presence of lamellar collision due to their curvature.

If we now compare the lamellar edge-on morphology found after crystallization of PLLA and PDLA for the same conditions of crystallization, there is a very distinct difference. For example, in Figure 2, two AFM pictures are depicted for two samples crystallized at 145 °C, for films having similar thicknesses, i.e., 14 and 16 nm.

At first sight, the two polymers exhibit exactly the same morphology, i.e., a bunch of edge-on lamellae irradiating from the nucleation line, surrounded by flat-on lamellae. However, a closer examination reveals that the curvature of the edge-on lamellae differs in these two cases. In PLLA, the edge-on lamellae exhibit an S shape whereas in PDLA, the edge-on lamellae have a Z shape. This difference is seen at all temperatures and thicknesses investigated here.

Figure 3 shows a close-up view in three dimensions of the two types of characteristic and isolated edge-on lamellae. Figure 3a exhibits an edge-on lamella which emerges from the melt before the crystallization of any flat-on lamella. In Figure 3b, we observe an edge-on lamella which emerges, surrounded by flat-on lamellae. In this case, the crystallization temperature was lower than in Figure 3a, and therefore, the lamella was quasi-instantly surrounded by flat-on dendritic crystals. But we can easily observe the edge-on lamella which emerges that time from the flat-on lamella. Using electron diffraction, it was verified that the crystal structures of PLLA and PDLA are the same.

It was not possible to verify the behavior of the racemic PLLA/PDLA mixture because it forms a stereocomplex, having a melting temperature 55 °C above that of pure PLLA and pure PDLA and having a different crystal structure.[26,27]

Discussion. The occurrence of lamellar twisting in polymer crystallization has been observed in several synthetic polymers. Even in polyethylene, it has been established that, in spherulites, dominant lamellae adopt an S-shaped profile.[23] This phenomenon appears to be more frequent with chiral polymers since their spherulites are frequently banded, implying that their lamellae twist. The most enlightening example is that of polyepichlorohydrin. In a first study, Singfield and Brown have demonstrated that the spherulites of pure poly(*S*-epichlorohydrin) or poly(*R*-epichlorohydrin) are banded contrary to the spherulites of the stereoblock copolymers or the polyenantiomer blends, which are nonbanded. The banding and the associated lamellar

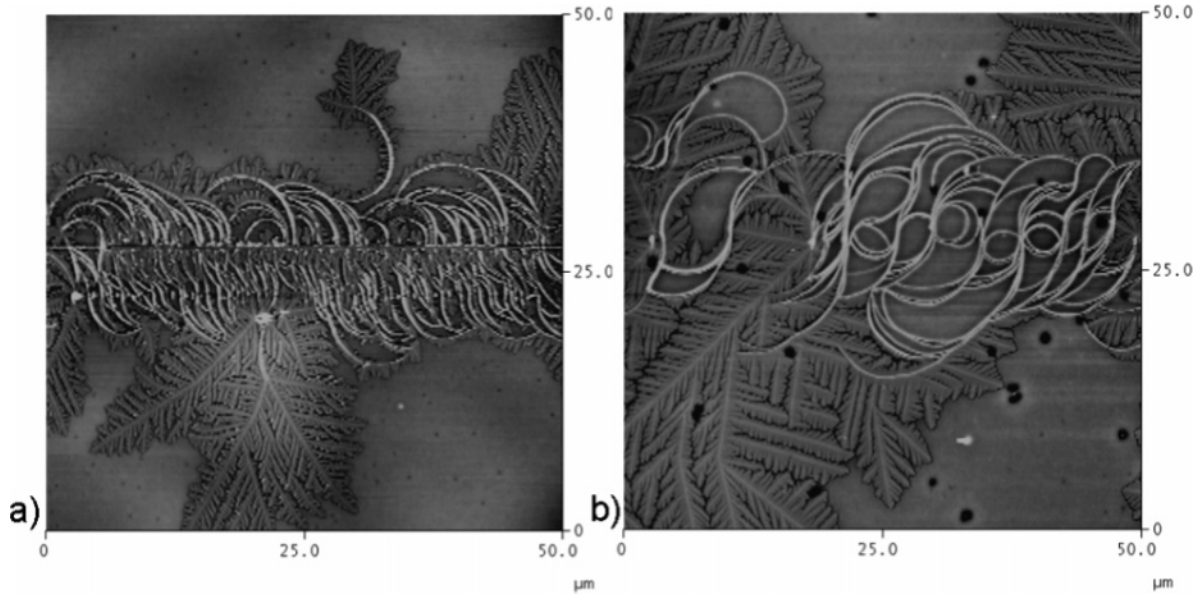

Figure 2. (a) 16 nm thick poly(D-lactide) film crystallized at 145 °C; (b) 14 nm thick poly(L-lactide) film crystallized at 145 °C. The two pictures exhibit edge-on and flat-on crystallizations. PDLA shows Z-shaped edge-on crystals and PLLA S-shaped edge-on crystals.

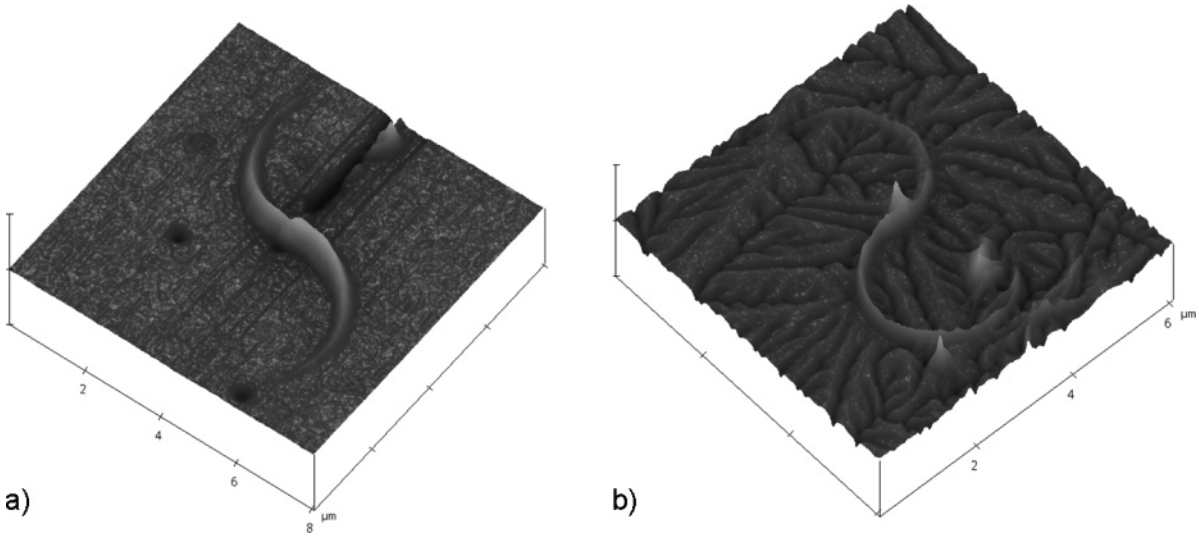

Figure 3. 3-D pictures of single edge-on lamellae in (a) PLLA 15 nm film crystallized at 160 °C (8 × 8 μm) and (b) PDLA 15 nm film crystallized at 125 °C (6 × 6 μm).

twist can be correlated with the presence of chirality.[28] A second study, based on AFM surface observations of the spherulites, has permitted to show a correlation between the chiral conformation of the polymer and the sense of twisting.[18] In this case, the chirality is clearly at the origin of lamellar twisting and twisting direction. Similarly, with chiral polyesters, Li, Lotz, and Cheng et al. have shown that the change of the handedness of the chiral center produces a reversal of the lamellar twist.[19−21]

The origin of lamellar twisting has been the subject of long-standing discussions. Basically, two explanations are currently considered: in the first one, the twisting is the global result, at least in polyethylene, of a succession of isochiral screw dislocations, with each screw dislocation contributing to the overall twist.[29−31] However, there are more and more evidences against this explanation. For example, in polyepichlorohydrin, Saracovan et al.[32] have observed the coexistence of both right- and left-handed screw dislocations in the two enantiomers (*R* and *S*), randomly. Recently, Xu et al.[33] have observed during the lamellar growth of poly(3-hydroxybutyrate-*co*-3-hydroxyhexanoate) lamellar twisting and screw dislocations using in situ AFM. The screw dislocations appear to be at the origin of the lamellar branching, but the lamellae twist before screw dislocations appear. This observation demonstrates that screw dislocations are not necessarily the cause of lamellar twisting in banded spherulites.

The second explanation, which is initially due to Keith and Padden,[23,24] ascribes the twisting observed to the presence of unbalanced surface stresses between the two surfaces of the lamella. Chain tilt, difference in fold volume, or asymmetry in fold environment (between the top and the bottom of the lamellae) could be at the origin of the stress unbalanced repartition. This explanation seems the more reasonable one at this moment, in view of all evidence available.[22]

In the present study, the motion of the AFM tip in contact with the amorphous film aligns chains along the probe scanning direction. That artificial alignment induces the nucleation with chains oriented parallel to the substrate, leading to an edge-on crystallization (the flat-on crystals have their chains perpendicular to the surface). Kikkawa et al.[12] have demonstrated that the edge-on polylactide lamellae grow along the *b* axis, the *c* axis being obviously parallel to the plane of the substrate.

In the edge-on crystals, the lamellar curvature radius depends on the temperature, as will be reported in a future paper, but its

direction only depends on the chirality. The correlation between the chirality of the chain and the helix conformation is well established; it is quasi-universal according to ref 22. However, the correlation between chirality and the sense of curvature (or twisting) of the lamellae is not general. It has been observed in a certain number of cases, i.e., with polyepichlorohydrins, but not in others.[22] For example, poly(3-hydroxyvalerate) and poly(3-hydroxybutyrate), which both exhibit a left-handed chain helix, lead to right- and left-handed lamellar twisting, respectively.[32] Similarly, polyesters with the same configuration of the chiral moiety but attached to paraffinic moieties with different lengths display right- or left-handed twist, depending on the paraffin segment length.[34] The case of polylactides is, in that context, an interesting example.

What can be in this case the physical origin of the curvature? In the context of Keith and Padden's suggestion, the observed edge-on lamellae can be considered as "half-lamellae" and the curvature the result of a different behavior of the two halves of the same lamella splitted along its center, induced by a stress unbalanced repartition.[23] It has been shown that the two half-lamellae resulting from a splitted lamella bend in different directions, as do the edge-on lamellae shown in Figures 2 and 3. However, the chain tilt cannot be considered as the origin of the unbalanced stress in this case, and another explanation must be sought.

In the literature, nylon-6,6 is one of the most interesting cases, in which the number of repeat units in the crystal is determined by the lamellar thickness and can affect the final configuration of the fold.[35] Three different configurations are possible: one where the folding on both sides of the lamellae are made of acid groups, one where both sides of the lamellae are made of amine groups, and finally one where one side exhibits amine folding and the other acid folding. The last case induces a lamellar scrolling due to a surface stress difference between the two sides. In the case of polylactides, the two polyenantiomers have the same chemical structure on both sides, but the sense of rotation of the chain helix is different. This difference presumably changes the exit angle of the chain fold from one polyenantiomer to the other and from one side to the other, creating an unbalanced surface stress between the two sides and causing the curvature.

In conclusion, the crystallization of thin polylactide films reveals a clear correlation between chain chirality and the macroscopic shape of edge-on crystals. The chirality leads to a lamellar curvature with a specific direction: with an S-shape in the case of PLLA and a Z-shape in the case of PDLA. This is another example demonstrating that the study of thin and ultrathin polymer films can reveal information on the crystallization characteristics of polymers which cannot be obtained in thick films or bulk phase.[36]

References and Notes

(1) Ray, S. S.; Okamoto, M. *Macromol. Rapid Commun.* **2003**, *24*, 815−840.

(2) Sarasua, J. R.; Prud'homme, R. E.; Wisniewski, M.; Borgne, A. L.; Spassky, N. *Macromolecules* **1998**, *31*, 3895−3905.

(3) Cartier, L.; Okihara, T.; Ikada, Y.; Tsuji, H.; Puiggali, J.; Lotz, B. *Polymer* **2000**, *41*, 8909−8919.

(4) Puiggali, J.; Ikada, Y.; Tsuji, H.; Cartier, L.; Okihara, T.; Lotz, B. *Polymer* **2000**, *41*, 8921−8930.

(5) Aleman, C.; Lotz, B.; Puiggali, J. *Macromolecules* **2001**, *34*, 4795−4801.

(6) Miyata, T.; Masuko, T. *Polymer* **1998**, *22*, 5515−5521.

(7) Hoogsteen, W.; Postems, A. R.; Pennings, A. J.; Brinke, G. T. *Macromolecules* **1990**, *23*, 634−642.

(8) Miyata, T.; Masuko, T. *Polymer* **1997**, *38*, 4003−4009.

(9) Sasaki, S.; Asakura, T. *Macromolecules* **2003**, *36*, 8385−8390.

(10) Kang, S.; Hsu, S. L.; Stidham, H. D.; Smith, P. B.; Leugers, M. A.; Yang, X. *Macromolecules* **2001**, *34*, 4542−4548.

(11) Kikkawa, Y.; Abe, H.; Iwata, T.; Inoue, Y.; Doi, Y. *Biomacromolecules* **2002**, *3*, 350−356.

(12) Kikkawa, Y.; Abe, H.; Fujita, M.; Iwata, T.; Inoue, Y.; Doi, Y. *Macromol. Chem. Phys.* **2003**, *204*, 1822−1831.

(13) Kikkawa, Y.; Abe, H.; Fujita, M.; Iwata, T.; Inoue, Y.; Doi, Y. *Biomacromolecules* **2001**, *2*, 940−945.

(14) Fujita, M.; Doi, Y. *Biomacromolecules* **2003**, *4*, 1301−1307.

(15) Nandi, N.; Vollhardt, D. *Chem. Rev.* **2003**, *103*, 4033−4075.

(16) Pasteur, L. *Ann. Chim. Phys.* **1848**, *24*, 442−459.

(17) Lotz, B.; Gonthier-Vassal, A.; Brack, A.; Magoshi, J. *J. Mol. Biol.* **1982**, *156*, 345−357.

(18) Singfield, K. L.; Klass, J. M.; Brown, G. R. *Macromolecules* **1995**, *28*, 8006−8015.

(19) Li, C. Y.; Cheng, S. Z. D.; Ge, J. J.; Bai, F.; Zhang, J. Z.; Mann, I. K.; Harris, F. W.; Chien, L.; Yan, D.; He, T.; Lotz, B. *Phys. Rev. Lett.* **1999**, *83*, 4558−4561.

(20) Li, C. Y.; Ge, J. J.; Bai, F.; Calhoum, B. H.; Harris, F. W.; Cheng, S. Z. D.; Chien, L.; Lotz, B.; Keith, H. D. *Macromolecules* **2001**, *34*, 3634−3641.

(21) Li, C. Y.; Jin, S.; Weng, X.; Ge, J. J.; Zhang, D.; Bai, F.; Harris, F. W.; Cheng, S. Z. D.; Yan, D.; He, T.; Lotz, B.; Chien, L. *Macromolecules* **2002**, *35*, 5475−5482.

(22) Lotz, B.; Cheng, S. Z. D. *Polymer* **2005**, *46*, 577−610.

(23) Keith, H. D.; Padden, F. J. *Polymer* **1984**, *25*, 28−42.

(24) Keith, H. D.; Padden, F. J. *Macromolecules* **1996**, *29*, 7776−7786.

(25) Lovinger, A. J.; Keith, H. D. *Macromolecules* **1996**, *29*, 8541−8542.

(26) Brizzolara, D.; Cantow, H. J.; Diedrichs, K.; Keller, E.; Domb, A. J. *Macromolecules* **1996**, *29*, 191−197.

(27) Tsuji, H.; Hyon, S.; Ikada, Y. *Macromolecules* **1992**, *25*, 2940−2946.

(28) Singfield, K. L.; Brown, G. R. *Macromolecules* **1995**, *28*, 1290−1297.

(29) Bassett, D. C.; Hodge, A. M. *Polymer* **1978**, *19*, 469.

(30) Bassett, D. C.; Hodge, A. M. *Proc. R. Soc. London* **1979**, *A359*, 121.

(31) Bassett, D. C.; Hodge, A. M. *Proc. R. Soc. London* **1981**, *A377*, 61.

(32) Saracovan, I.; Cox, J. K.; Revol, J. F.; Manley, R. S. J.; Brown, G. R. *Macromolecules* **1999**, *32*, 717−725.

(33) Xu, J.; Guo, B.; Zhang, Z.; Zhou, J.; Jiang, Y.; Yan, S.; Li, L.; Wu, Q.; Chen, G.; Schultz, J. M. *Macromolecules* **2004**, *37*, 4118−4123.

(34) Li, C. Y.; Cheng, S. Z. D.; Weng, X.; Ge, J. J.; Bai, F.; Zhang, J. Z.; Calhoum, B. H.; Harris, F. W.; Chien, L.; Lotz, B. *J. Am. Chem. Soc.* **2001**, *123*, 2462−2463.

(35) Cai, W.; Li, C. Y.; Li, L.; Lotz, B.; Keating, M.; Marks, D. *Adv. Mater.* **2004**, *16*, 600−605.

(36) Mareau, V. H.; Prud'homme, R. E. In *Soft Materials*; Marangoni, A. G., Ed.; Marcel Dekker: New York, 2005; pp 39−71.

MA060316C